Modeling of Germanium-Based Perovskite Solar Cell for Different Hole Transport Materials and Defect Density

Nurul Afiqah Buruhanutheen[1], Ahmad Sharmi Abdullah[1], Mohd Halim Irwan Ibrahim[2], Fauzan Ahmad[3] and Mohd Haniff Ibrahim[*1]

[1]*Faculty of Electrical Engineering, Universiti Teknologi Malaysia, Johor, Malaysia*
[2]*Faculty of Mechanical and Manufacturing Engineering, Universiti Tun Hussein Onn Malaysia, Johor, Malaysia*
[3]*Malaysia-Japan International Institute of Technology (MJIIT), Kuala Lumpur, Malaysia*

Received August 16, 2023; accepted September 27, 2023; published September 30, 2023

Abstract—The performance of four distinct materials (organic and inorganic) was simulated and analyzed as hole transport layer (HTL) in the design of germanium (Ge)-based Perovskite Solar Cell (PSC). A 1-dimensional numerical software (SCAPS 1-D) has been applied to simulate the HTL candidates: spiro-OMeTAD, PTAA, nickel oxide (NiO), and copper (I) thiocyanate (CuSCN), with tin (IV) dioxide (SnO2) as the electron transport layer (ETL). The thickness of the methylammonium germanium iodide ($CH_3NH_3GeI_3$) absorber varied from 300 nm to 1100 nm, and the highest simulated power conversion efficiency was achieved at 800 nm for all HTL candidates. It was observed that the inorganic CuSCN outperformed its counterparts with a power conversion efficiency (PCE) of 25.38%. The effect of the perovskite absorber's defect density was investigated, and ultimately, it was demonstrated that this value is disproportionately related to the PCE. A reduction of nearly 98% in PCE was recorded when the defect density increased from 1×10^{14} cm^{-3} to 1×10^{20} cm^{-3}. Additionally, for a constant ETL thickness of 80 nm, it was revealed that the PCE would decrease slightly, ranging from 0.1% to 0.3%, with an increase in HTL thickness from 50 nm to 300 nm. Comparing the PCE of our current work with published reports further justifies its competitiveness.

Solar cells represent the future of sustainable energy for human civilization. Significant energy production will be required to sustain and enhance our future standard of living. Fortunately, advances in science and technology have enabled us to harness solar energy as an alternative source to help meet the growing demand. Solar energy technologies utilize the concept of solar radiation to convert sunlight into electrical energy. Research into the fundamental concept of the photovoltaic effect for solar energy generation was conceptualized in 1839 by Alexandre-Edmond Becquerel [1]. Since then, numerous research efforts have been dedicated to investigating material properties aimed at achieving higher power conversion efficiency (PCE).

Up to now, organic-inorganic halide Perovskite Solar Cell (PSC), categorized as third-generation solar cells, have garnered significant interest since their initial conception and proof of concept demonstration by Kojima *et al*. in 2009 [2]. The prominent advantages of PSC, which include high absorption coefficients, tunable bandgaps, extended carrier diffusion lengths, long carrier lifetimes, and high carrier mobilities [3], have contributed to this extensive interest. However, the instability and toxicity of the lead (Pb) element in perovskite may jeopardize its potential for use in large-scale commercial production. Hence, there is a need to seek an alternative candidate to replace the Pb element with minimal sacrifice to the PCE. We note that few efforts have been initiated to replace the Pb element in perovskite by using tin (Sn) [4–9] and germanium (Ge) [10–12] due to their belonging to the same subgroup. However, a performance comparison for diverse hole transport layer (HTL) materials ranging from organic to inorganic elements is still lacking. Notably, the HTL extensively contributes to the efficiency and performance of PSC, particularly in facilitating hole transportation from the absorber to the back contact [4]. Indeed, selecting the optimal HTL materials is crucial for developing highly efficient PSC.

In this letter, we report on using methyl ammonium germanium iodide ($CH_3NH_3GeI_3$) as the absorber material, along with four potential HTL candidates. These include organic-based 2,2',7,7'-Tetrakis[N,N-di(4-methoxyphenyl)amino]-9,9'-spiro bi fluorene (spiro-OMeTAD) and poly[bis(4-phenyl)(2,4,6-trimethylphenyl)amine] (PTAA), as well as inorganic candidates: nickel oxide (NiO) and copper (I) thiocyanate (CuSCN). Please note that the utilization of these four HTM candidates for Sn-based perovskite ($CH_3NH_3SnI_3$) has been previously demonstrated in a handful of publications [4–9]. Furthermore, tin (IV) dioxide (SnO_2) has been chosen as the electron transport layer (ETL) for this study based on its established capacity to achieve a higher PCE, as demonstrated in our previous work in [9]. We believe that the comparative analysis conducted in this study can serve as the foundation for selecting suitable materials for realizing the Ge-based PSC. The effect of the absorber's defect density will be comprehensively investigated, as it can lead to carrier recombination and affect carrier lifetime.

The primary tool applied in this study will be the SCAPS 1-D modeling software, based on the numerical solution of Poisson's equation and continuity equations for electrons and holes. The solar illumination is internally generated at AM 1.5G ($1000Wm^{-2}$) [9]. Figure 1 shows the planar n-i-p cross-section structure of our

* E-mail: mohdhaniff@utm.my

modeled Ge-based PSC. It consists of gold (Au) as the metal back contact and fluorine-doped tin oxide (FTO) as the front contact. Four candidates for the HTM are indicated.

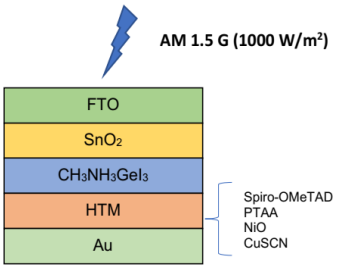

Fig. 1. Planar n-i-p Ge-based PSC.

The energy band diagram for each layer of the simulated structure is depicted in Fig. 2, while the properties of all materials used in this work are tabulated in Table 1. This information has been extracted from various sources [3–12].

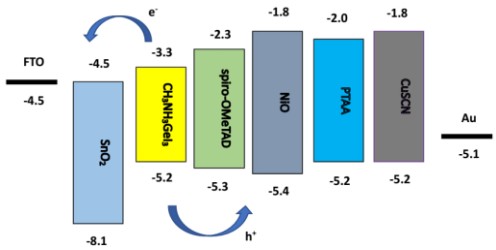

Fig. 2. Energy band diagram in eV unit.

Table 1. Material properties for simulated PSC.

Properties	FTO	SnO_2	$CH_3NH_3GeI_3$	Spiro-MeOTAD	PTAA	NiO	CuSCN
Thickness(nm)	500	80	300-1100	200	200	200	200
Bandgap (eV)	4.5	3.6	1.9	3.0	3.2	3.6	3.4
Affinity (eV)	4.0	3.98	4.17	2.05	2.1	1.46	2.1
Dielectric Permittivity	9	8	10	3	3	10.7	10
DOS_{CB} (cm^{-3})	$2.2x10^{18}$	$3.16x10^{18}$	$1x10^{16}$	$2.8x10^{19}$	$2.2x10^{18}$	$2.8x10^{19}$	$2.5x10^{18}$
DOS_{VB} (cm^{-3})	$1.8x10^{19}$	$2.5x10^{19}$	$1x10^{15}$	$1x10^{19}$	$1x10^{19}$	$1x10^{19}$	$1.8x10^{19}$
μ_e (cm^2/Vs)	20	15	$162 x10^3$	$1 x10^{-4}$	$2 x10^{-3}$	12	$2 x10^{-4}$
μ_h (cm^2/Vs)	10	0.1	$101 x10^3$	$2 x10^{-4}$	$4 x10^{-3}$	2.8	1
Acceptor Concentration (cm^{-3})	0	0	$1x10^9$	$1x10^{18}$	$1x10^{19}$	$1x10^{18}$	$1x10^{18}$
Donor Concentration (cm^{-3})	$2x10^{19}$	$1x10^{19}$	$1x10^9$	0	$1x10^{18}$	0	0

It is essential to determine the optimal thickness of the perovskite absorber. This knowledge will ultimately maximize carrier generation and photocurrent, resulting in the highest possible PCE. To achieve this goal, we have varied the thickness of the perovskite absorber across the range of 300 to 1100 nm. Simultaneously, we maintained the thickness of the other layers at a constant level, as established by our previous simulation in [9]. Figures 3–6 depict the variations in short circuit current (J_{sc}), open circuit voltage (V_{oc}), fill factor (FF), and PCE concerning the thickness of the absorber for all HTL materials, respectively. From these figures, it becomes evident that the FF experiences a decrease with an increase in the absorber thickness. Conversely, the J_{SC} increases due to enhanced carrier generation in the absorber as its thickness grows, causing the PCE to rise until it saturates at 800 nm. It is important to note that the amount of carrier generation in the absorber is directly proportional to its thickness. However, beyond a certain point, a thicker absorber will lead to carrier saturation, resulting in no further increase in the current generation.

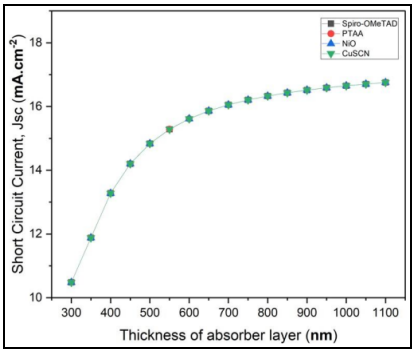

Fig. 3. Absorber thickness variation with J_{sc}.

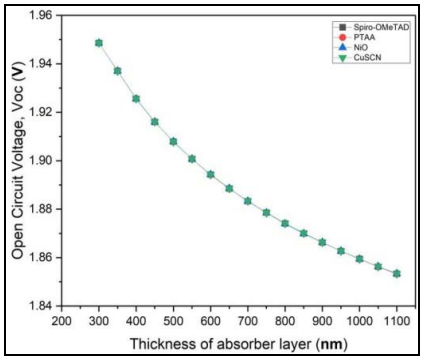

Fig. 4. Absorber thickness variation with V_{oc}.

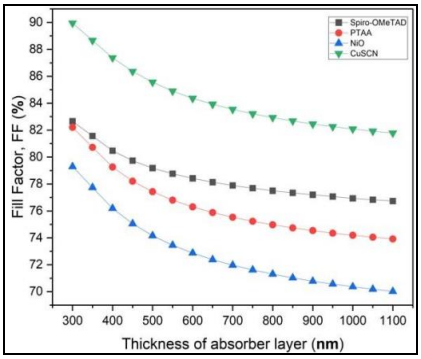

Fig. 5. Absorber thickness variation with FF.

Based on our extensive simulations, we have identified 800 nm as the optimal thickness for the absorber, resulting in PCE values of 23.72% (spiro-OMeTAD), 22.94% (PTAA), 21.82% (NiO), and 25.38% (CuSCN). This indicates that the inorganic CuSCN exhibits superiority compared to the other organic and inorganic

HTL candidates. The above simulation is based on an absorber defect density value of 1×10^{14} cm^{-3}.

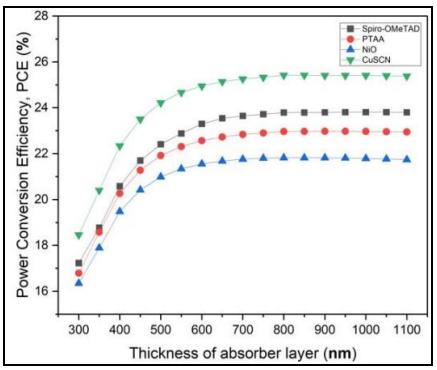

Fig. 6. Absorber thickness variation with PCE.

These defects can take the form of structural flaws and irregularities within material lattice structure. This is a crucial parameter to consider since it can significantly impact the performance of PSC. The simulation has been carried out to examine its effect using spiro-OMeTAD and CuSCN as HTL for defect density values ranging from 1×10^{14} to 1×10^{20} cm^{-3}. The graph depicting the variation in PCE with these changes is shown in Fig. 7. The diagram illustrates a clear trend: as the defect density increases, the PCE values decrease for both HTL candidates. Quantitatively, the PCE reduces by approximately 98% for both HTL candidates within the calculated range.

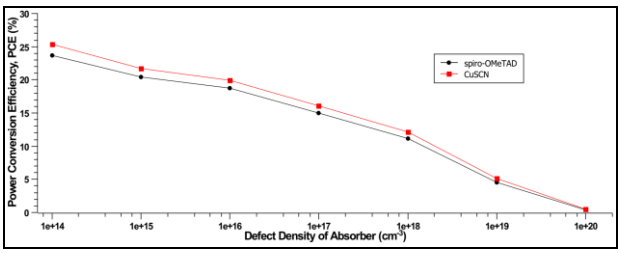

Fig. 7. PCE variation against absorber defect density.

Subsequently, the PCE performance is evaluated by varying the thickness of these HTL candidates while keeping the ETL thickness constant at 80 nm and the absorber thickness at 800 nm. The results are illustrated in Fig. 8. The findings reveal a marginal reduction of 0.1% to 0.3% in PCE due to the HTL thickness variation from 50 nm to 300 nm. These observations are consistent with previous reports [9, 12] on variations in the transport layer thickness. This phenomenon is primarily attributed to the slight increase in carrier recombination that occurs with greater HTL thickness.

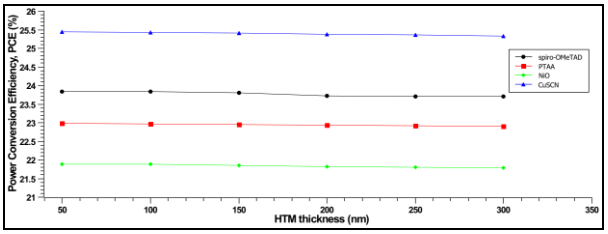

Fig. 8. HTL thickness variation with PCE.

Finally, a comparison has been made with published reports on lead-free perovskite (Sn-based and Ge-based) to justify the competitiveness of our current work. This comparison has been presented in Table 2. Based on the recorded PCE values, it is evident that our proposed work, particularly utilizing CuSCN as the HTL and SnO_2 as the ETL, performs competitively better compared to other combinations. However, despite this being a simulation study, the information gathered may be considered a significant effort, especially in aiding further PSC development based on Ge-based perovskite.

Table 2. Comparison between this work and previous reports.

Solar cell structure [reference]	Voc (V)	Jsc (mA/cm^2)	FF (%)	PCE (%)
FTO/TiO_2/$CH_3NH_3SnI_3$/Cu_2O/Au [7]	0.66	42.70	69.82	18.36
FTO/ZnO NP/ $CH_3NH_3SnI_3$/CuSCN/Au [8]	0.89	32.8	79.65	23.51
FTO/ZnO NP/ $CH_3NH_3SnI_3$/NiO/Au [8]	0.77	32.05	77.83	19.27
FTO/TiO_2/$CH_3NH_3GeI_3$/NiO/Au [10]	1.93	13.91	74.97	19.30
FTO/TiO_2/$CH_3NH_3GeI_3$/Cu_2O/Au [10]	1.92	14.20	79.28	21.60
FTO/CuSCN/ $CH_3NH_3GeI_3$/C_{60}/Ag [11]	1.17	26.53	69.38	21.60
FTO/TiO_2/$CH_3NH_3GeI_3$/Spiro-OMeTAD/Au [12]	1.14	13.22	73.07	11.05
FTO/SnO_2/$CH_3NH_3GeI_3$/CuSCN/Au [this work]	1.87	16.33	82.93	25.38

The authors acknowledged Dr Marc Burgelman from the University of Gent, Belgium, for providing the SCAPS-1D.

References

[1] W.R. Becquerel, J. Chem. Phys. **5**, 1505 (1960).
[2] A. Kojima, K. Teshima, Y. Shirai, T. Miyasaka, J. Am. Chem. Society **131**, 6050 (2009).
[3] M.M. Salah, K.M. Hassan, M. Abouelatta, A. Shaker, Optik **178**, 958 (2019).
[4] S. Rai, B. Pandey, A. Garg, D. Dwivedi, Opt. Mat. **121**, 111645 (2021).
[5] H. Liangsheng, Z. Min, S. Yubao, M. Xinxia, W. Jiang, Z. Qunzhi, F. Zaiguo, L. Yihao, H. Guoyu, L. Tong, Solar Energy, **230**, 345 (2021).
[6] K. Fatema, M. Arefin, Opt. Mat. **125**, 112036 (2022).
[7] P. Patel, Scien. Rep. **11**, 3082 (2021).
[8] P. Roy, Y. Raoui, A. Khare, Opt. Mat. **125**, 112057 (2022).
[9] A.I. Azmi, M.Y. Mohd Noor, M.H.I. Ibrahim, F. Ahmad, M.H. Ibrahim, Jordan J. Electron. Eng. **8**, 355 (2022).
[10] A.A. Kanoun, M.B. Kanoun, A.E. Merad, S. Goumri-Said, Solar Energy, **182**, 237 (2019).
[11] A. Hima, N. Lakhdar, Opt. Mat. **99**, 109607 (2020).
[12] S.T. Jan, M. Noman, Solar Energy **237**, 29 (2022).

